ISSN 0023-1584, Kinetics and Catalysis, 2012, Vol. 53, No. 4, pp. 504–510. © Pleiades Publishing, Ltd., 2012.
Original Russian Text © T.P. Minyukova, A.A. Khassin, N.A. Baronskaya, L.M. Plyasova, V.V. Kriventsov, E. S. Rozhko, G.A. Filonenko, T.M. Yurieva, 2012, published in Kinetika i Kataliz, 2012, Vol. 53, No. 4, pp. 527–533.

High-Temperature Water Gas Shift Catalyst Based on Nanodisperse, Metastable, Partially Hydrated Iron Oxide—Two-Line Ferrihydrite

T. P. Minyukova[a,b,*], A. A. Khassin[a,b], N. A. Baronskaya[a,b], L. M. Plyasova[a,b], V. V. Kriventsov[a], E. S. Rozhko[a,b], G. A. Filonenko[a,b], and T. M. Yurieva[a]

[a] *Boreskov Institute of Catalysis, Siberian Branch, Russian Academy of Sciences, Novosibirsk, 630090 Russia*
[b] *Novosibirsk State University, Novosibirsk, 630090 Russia*
* *e-mail: min@catalysis.ru*

Received November 30, 2011

Abstract—Two-line ferrihydrite (2L-FH) is a metastable, heavily disordered, partially hydrated Fe(III) oxide. The catalyst prepared by heat treatment of 2L-FH promoted with chromium ions (~9 at %) and copper ions (4–7 at %) is much more active in the water gas shift (WGS) reaction at low temperatures (<350°C) than the conventional Fe-containing catalysts. According to XAFS spectroscopy data, the copper cations in 2L-FH are in the Cu^{2+} state and are in a tetragonally distorted octahedral environment, while under the WGS conditions at <350°C, copper is in the reduced state, specifically, in the form of ultrafine (<2 nm) Cu^0 particles. It is due to these particles that the catalyst is very active below 350°C. Above 400°C, the Cu^0 particles are deactivated under the reaction conditions and the catalytic activity is only due to iron active sites, whose number is proportional to the specific surface area of the catalyst. The specific activity of the catalyst at these temperatures is close to the activity of the conventional (hematite-based) WGS catalysts. The high activity of the 2L-FH-based catalyst at <350°C makes it possible to reduce the starting temperature of the adiabatic high-temperature WGS reactor.

DOI: 10.1134/S0023158412040064

Two-line ferrihydrite (2L-FH) is a metastable, heavily disordered, partially hydrated Fe(III) oxide of variable composition $Fe_2O_{3-0.5y}(OH)_y \cdot nH_2O$ ($0 \le y \le 1.96$) in which, according to many authors, over 4% of the O^{2-} anions are replaced by OH groups [1–3]. There are several methods of synthesizing ferrihydrite. Depending on its degree of crystallinity, it is called two- or six-line ferrihydrite, according to the number of peaks in its X-ray diffraction pattern. A typical diffraction pattern of 2L-FH is presented in Fig. 1. Figure 2 shows a high-resolution micrograph of 2L-FH [4].

The crystallite size of 2L-FH is 1.6–2.0 nm, and its specific surface area is 300–400 m^2/g, so this material is expected to have a high catalytic activity and a high adsorption capacity. It can also be anticipated that, since its crystallites are nanosized, 2L-FH will possess unique catalytic properties differing from those of well-crystallized iron oxides, such as α-Fe_2O_3 (hematite) and α-FeOOH (goethite). An analysis of publications on the catalytic properties of 2L-FH-based catalysts in the Fischer–Tropsch synthesis [5–7], coal liquefaction [8, 9], and WGS reaction [10–12] suggests that this material is very promising for catalysis. The possible risk in its application stems from its metastability. Since the dehydration and subsequent crystallization of ferrihydrite into hematite are kinetically controlled processes, they can proceed at a low rate even at room temperature. Metastable materials are usable either in fast processes or at low temperatures and either in the promoted state or as a precursor of an active component. The possibility of enhancing the thermal stability of 2L-FH by promotion makes this

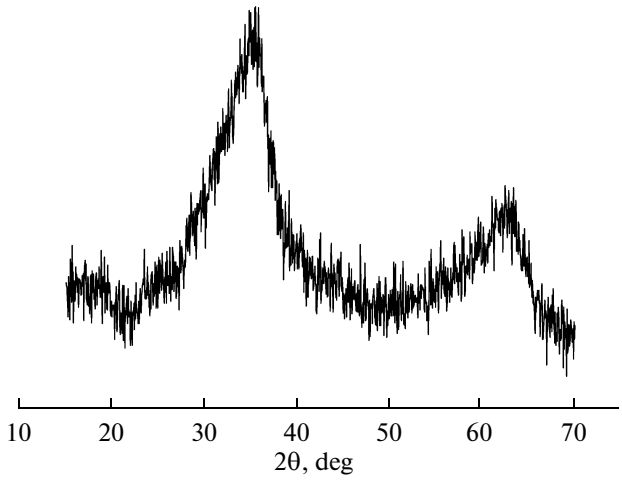

Fig. 1. Diffraction pattern of 2L-FH promoted with Cr^{3+} (Fe^{3+} : Cr^{3+} = 10 : 1).

material promising both as a catalyst precursor and as a catalyst and adsorbent.

Here, we report the effect of promotion with Al, Cr, and Cu ions on the thermal stability and dehydration and recrystallization kinetics of 2L-FH and discuss the nature of the activity of 2L-FH promoted with Cu and Cr ions in the WGS reaction below 350°C.

EXPERIMENTAL

Catalyst Preparation

Hydroxo compounds of preset composition were precipitated from nitrate solutions by adding a sodium carbonate solution. The precipitate was washed by decantation. The catalyst mass was dried and calcined in flowing nitrogen at 200–300°C. The designations and chemical and phase compositions of the samples examined are listed in Table 1.

Phase analysis

X-ray diffraction patterns were obtained on a D-500 diffractometer (Siemens) equipped with a high-temperature attachment for in situ studies [13]. This attachment allowed X-ray diffraction experiments to be conducted in controllable gas media (air, inert gas, H_2, $H_2 + H_2O$) at temperatures of up to 350°C. The sample chamber was purged with helium, and a He : H_2 : H_2O= 90 : 5 : 5 (vol %) mixture was then fed into it at a rate of 25 cm^3/s. The sample heating rate was 5 K/min. The sample was kept for 30 min at each preset temperature point, and a diffraction pattern was then recorded. Graphite-monochromated CuK_α radiation was used, with the monochromator placed in the reflected beam. Diffraction patterns were recorded in the $2\theta = 10$–70 deg range by point-by-point scanning with $2\theta = 0.05$ deg increments and a counting time of 5 s per point. Phases were identified using the ICDD PDF-2 database.

Differential Thermal Analysis (DTA)

Dehydration data for the materials were obtained by thermal analysis on a Netzsch STA-409 system in flowing argon at a sample heating rate of 10–20 K/min.

Determination of the Number of Active Fe Sites on the Surface

The active site quantification technique was based on the ability of the iron ions to undergo reversible reduction and oxidation under the action of a hydrogen-containing gas and N_2O, respectively, via the following reactions:

$$Fe^{3+} + H_2 = Fe^{2+} + 2H^+,$$
$$N_2O + 2Fe^{2+} = N_2 + 2Fe^{3+} + O^{2-}.$$

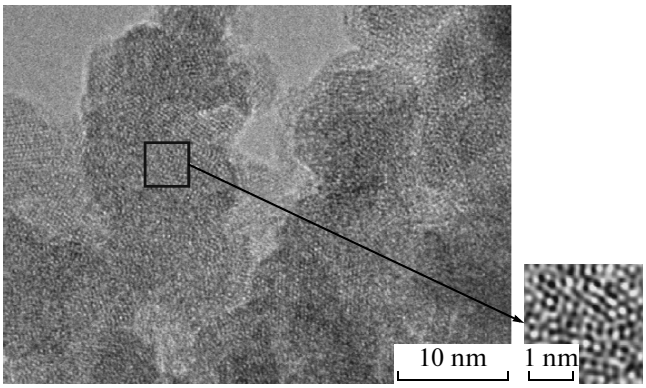

Fig. 2. HRTEM image of 2L-FH promoted with Cr^{3+}. The image on the right is the result of Fourier filtering.

The composition of the reducing mixture was adjusted so as to prevent the reduction of Fe^{3+} to Fe^0. This was done by adding water vapor to the hydrogen containing gas (3–4 vol % H_2 in Ar, H_2O : $H_2 = 1 : 1$). The oxidation reaction was carried out by pulsed titration with N_2O at 60°C. In the processing of the results of these experiments, we subtracted the fraction of N_2O spent on the oxidation of Fe^{2+} from the sample volume.

EXAFS and XANES Spectroscopy

Extended X-ray absorption fine structure (EXAFS) and X-ray absorption near-edge structure (XANES) spectra (Cu-*K*, Cr-*K*, Fe-*K*) were recorded on an EXAFS spectrometer (Siberian Synchrotron Radiation Center, Novosibirsk, Russia) using the transmission technique. After catalytic activity measurements, the sample was taken out of the reactor under flowing argon and was sealed in a tube filled with an inert gas. The atomic radial distribution function (RDF) was

Table 1. Designations and chemical and phase compositions of the materials examined

Designation	Chemical composition, at %	Phase composition
2L-FH	100% Fe^{3+}	Ferrihydrite
2L-FH(Al9)	91% Fe^{3+}, 9% Al^{3+}	Ferrihydrite
2L-FH(Cr9)	91% Fe^{3+}, 9% Cr^{3+}	Ferrihydrite
2L-FH(Cr9Cu7)	86% Fe^{3+}, 9% Cr^{3+}, 7% Cu^{2+}	Ferrihydrite
Goeth-Fe	100% Fe^{3+}	Goethite (FeOOH)
Hem-Fe	100% Fe^{3+}	Hematite (Fe_2O_3)

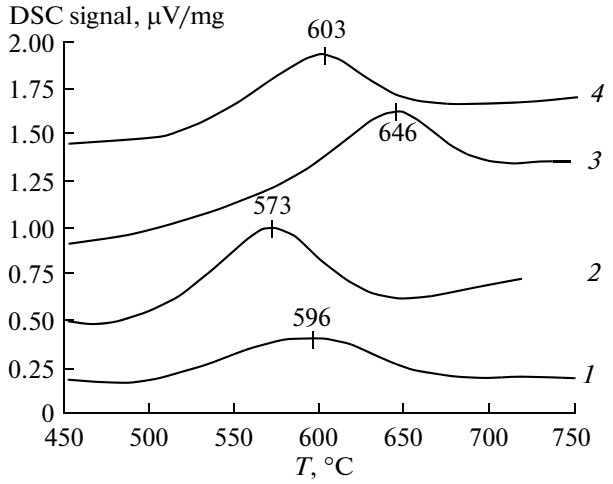

Fig. 3. DTA profiles for (*1*) 2L-FH, (*2*) 2L-FH(Al9), (*3*) 2L-FH(Cr9), and (*4*) 2L-FH(Cr9Cu7) heated at a rate of 20 K/min in flowing argon.

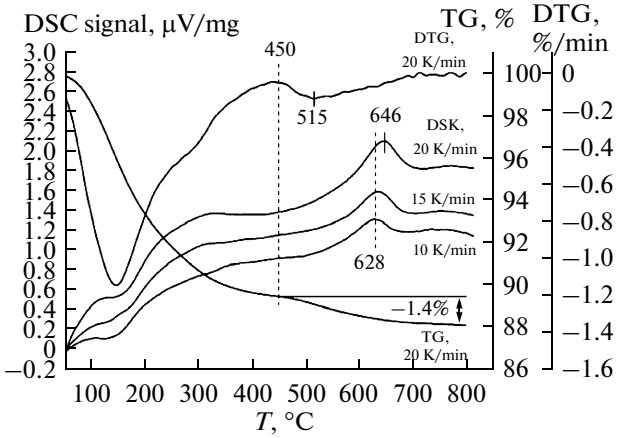

Fig. 4. TG, DTG, and DSC profiles for 2L-FH(Cr9) heated at different rates.

obtained using a Fourier transform ($k\chi(k)$) module in the wave number range from 2 to 12.0 $Å^{-1}$. Structural information (interatomic distances, coordination numbers, Debye factors) was gained by modeling the spectra using the EXCURV92 program [14] after Fourier filtration using available X-ray crystallographic data for reference compounds (Cu foil, CuO, and Cu_2O).

Catalytic Tests

The catalytic activity of the materials in the WGS reaction was measured in a flow reactor at 300–480°C and atmospheric pressure. The composition of the reaction mixture was $CO : CO_2 : H_2 = 12 : 5.5 : 82.5$ (vol %), and the steam-to-gas ratio was 0.6–0.9. The catalyst was used either in the form of 0.25–0.5 mm particles mixed with quartz glass of the same size fraction (1 : 1) or in the form of heat-conducting composite plates (HCCPs) as 25 × 2.5 mm disc segments. (For HCCP preparation and testing details, see [15]).

RESULTS AND DISCUSSION

Promoter Effect on the Thermal Stability of Ferrihydrite

The thermal behavior of 2L-FH promoted with Al, Cr, and Cu ions was studied by thermal analysis. The DTA curves of the 2L-FH samples heated at a rate of 20 K/min in flowing argon are presented in Fig. 3. Clearly, the promoters change the position of the exothermic peak corresponding to the crystallization of the hematite phase. The introduction of aluminum ions shifts the maximum of the exotherm from 596 to 573°C. The introduction of chromium ions shifts the exotherm to a higher temperature of 646°C. From the ferrihydrite → hematite transition peak positions determined at different heating rates, it is possible to calculate kinetic parameters of this phase transition. By way of example, we present the DSC curves recorded for the 2L-FH(Cr9) sample in argon at heating rates of 10, 15, and 20 K/min (Fig. 4). As the heating rate is increased, the exothermic peak shifts from 628 to 646°C.

Kinetic parameters were determined using the Netzsch thermokinetics program. The Ozawa–Flynn–Wall model-free method was employed, which enabled to estimate kinetic parameters without making any assumptions as to the reaction mechanism. The parameters were also determined by finding the kinetic model that describes the reaction mechanism most precisely. The best fit was provided by the Avrami–Erofeev model, in which the phase transition is assumed to be a first-order reaction. Table 2 presents the results of this kinetic data processing.

The kinetic parameters of the phase transition (activation energy and preexponential factor) determined by these methods for the promoted 2L-FH samples are in satisfactory agreement. For this reason, they were used to calculate the rate constant and rate of the ferrihydrite → hematite transition under isothermal conditions. This allowed us to determine the half-life of the promoted ferrihydrites (Table 3). It is evident that the Cr- and CrCu-promoted ferrihydrites are the most stable in the inert atmosphere.

Phase Composition of the Ferrihydrites Treated with a Reductive Gas Medium

The 2L-FH(Cr9Cu7) sample calcined at 240°C in argon was characterized by in situ X-ray diffraction in the $He : H_2 : H_2O = 90 : 5 : 5$ (vol %) gas medium. Fig-

Table 2. Kinetic parameters of the phase transition in the promoted 2L-FH materials

Ferrihydrite	T_{max}*, °C	Ozawa–Flynn–Wall method (for 50% conversion)		Avrami–Erofeev model	
		E_a, kJ/mol	log$A$, [s^{-1}]	E_a, kJ/mol	log$A$, [s^{-1}]
2L-FH	570	154	7.2	164	7.8
2L-FH(Al9)	537	110	4.6	99	4.0
2L-FH(Cr9)	628	288	14.7	289	14.6
2L-FH(Cr9Cu7)	582	218	11.1	217	11.1

* Position of the exothermic peak due to crystallization at a heating rate of 10 K/min.

ure 5 shows the diffraction patterns of the sample exposed to the reductive medium at different temperatures. As the temperature is raised to 300°C, the crystallization of a spinel phase (chromium ion–promoted Fe_3O_4) takes place and copper metal appears. At 350°C, the diffraction pattern indicates the presence of traces of hematite, α-Fe_2O_3. The diffraction pattern of the sample that was reduced at 350°C and was then exposed to air is different: it shows only peaks from the spinel phases and no reflections from the copper metal and hematite phases. Therefore, the copper metal particles existing in the reaction medium at 300–350°C are very reactive and oxidize readily when exposed to air.

State of Copper in 2L-FH(Cr9Cu7)

The state of copper was investigated by XAFS spectroscopy. Figure 6 shows the XANES spectra of the 2L-FH(Cr9Cu7) sample and reference materials: Cu foil, Cu_2O, and CuO. Copper in the initial catalyst sample is mainly in the form of Cu^{2+} cations in a distorted octahedral oxygen environment.

The atomic radial distribution curves (Fig. 7) indicate that, after the completion of the reaction at 340°C, the catalyst is a complicated multiphase nanosystem containing Cu^0 and Cu(II) oxides with a characteristic particle size of 2–3 nm. The interatomic distance and coordination number data for the reference samples and for 2L-FH(Cr9Cu7) are listed in Table 4.

Catalytic Properties of the Ferrihydrites

Table 5 lists steady-state reaction rate constants (determined after 140-h-long operation) for 2L-FH(Cr9Cu7) as HCCPs at 330°C before and after heat treatment at 480°C. For comparison, we present the activity of the conventional hematite-based catalyst (Hem-Fe). The 2L-FH(Cr9Cu7) sample that was not overheated in the reaction medium is far more active than the same sample heat-treated at 480°C or Hem-Fe. It is likely that the higher activity of 2L-FH(Cr9Cu7) below 350°C is due to the existence of ultrafine copper metal particles in this copper-promoted catalyst. As this catalyst is kept at 480°C, the copper particles undergo deactivation and the activity of the catalyst begins to be determined by the iron sites, as in the case of the conventional Fe-containing catalysts.

Table 6 lists steady-state rate constants for the reaction occurring under kinetic control at 340°C over the catalysts heat-treated at 480°C in the reaction medium, the surface concentrations of iron active sites determined by titration with N_2O, and catalytic activities per iron active site. Note that, under these conditions, the copper sites are inactive. Clearly, the number of Fe^{2+} active sites (AS) in the catalyst activated at 480°C is proportional to the specific surface area S_{sp} and is independent of the structure of the precursor compound. The catalysts prepared from precursors

Table 3. Half-lives of the promoted ferrihydrites at different temperatures

Ferrihydrite	Half-life, year		
	290°C	320°C	350°C
2L-FH	10	1.1	0.2
2L-FH(Al9)	7×10^{-3}	2×10^{-3}	8×10^{-4}
2L-FH(Cr9)	35600	1600	97
2L-FH(Cr9Cu7)	363	24	2

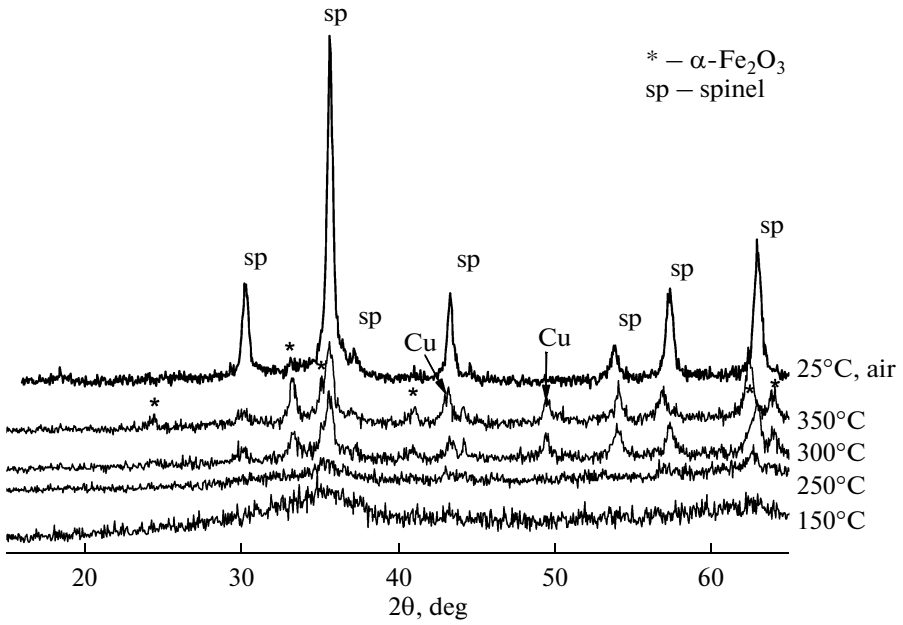

Fig. 5. In situ diffraction patterns of 2L-FH(Cr9Cu7) in the He : H_2 : H_2O = 90 : 5 : 5 (vol %) reductive atmosphere.

differing in their composition and structure show approximately equal WGS activities per active site.

CONCLUSIONS

The thermal stability of the ferrihydrite-type iron oxohydroxo compound can be significantly changed by introducing promoting ions. This provides means to make the ferrihydrite a more stable catalyst and adsorbent.

The WGS catalyst prepared from ferrihydrite promoted with copper and chromium ions shows an increased activity below 350°C. As the temperature is raised, the activity of this catalyst decreases irreversibly to become similar to the activity of copper-free ferrihydrite.

The number of iron active sites in the reduced catalysts based on the iron oxohydroxo compounds, both unpromoted and promoted, with a hematite, goethite, or ferrihydrite structure, is proportional to the specific surface area of the catalyst. The catalysts prepared from precursors differing in their composition and structure show approximately equal activities per Fe site.

Table 4. XAFS data characterizing the local environment of Cu atoms in Cu-containing materials (R = distance, N = coordination number; Debye–Waller factors are fixed at 0.009–0.012)

Neighbor atoms	CuO		Cu foil		2L-FH(Cr9Cu7) after reaction at 340°C	
	R, Å	N	R, Å	N	R, Å	N
Cu–O	1.95	4.0	–	–	1.93	2.9
Cu–Cu	–	–	2.56	12.0	2.55	4.5
Cu–Cu	2.95	4.0	–	–	–	–
Cu–Cu	3.40	2.1	–	–	–	–
	3.65	2.0	–	–	–	–

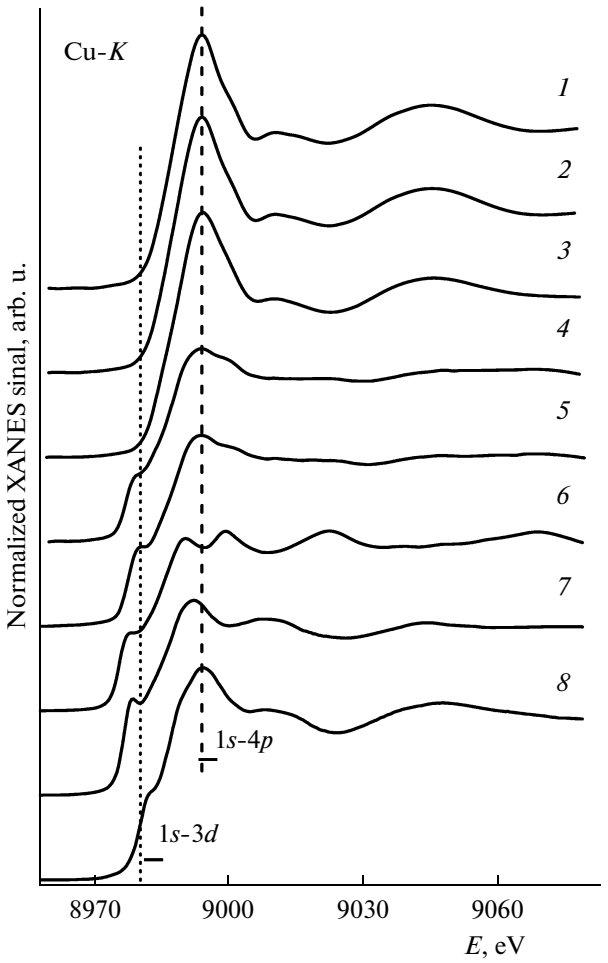

Fig. 6. Normalized XANES (Cu-*K*-edge) spectra: (*1*) 2L-FH(Cr9Cu7), dry; (*2*) 2L-FH(Cr9Cu7), 400°C; (*3*) 2L-FH(Cr9Cu7), 750°C; (*4*) 2L-FH(Cr9Cu7), 340°C, after reaction; (*5*) 2L-FH(Cr9Cu7), 480°C, after reaction; (*6*) Cu foil; (*7*) Cu_2O; (*8*) CuO.

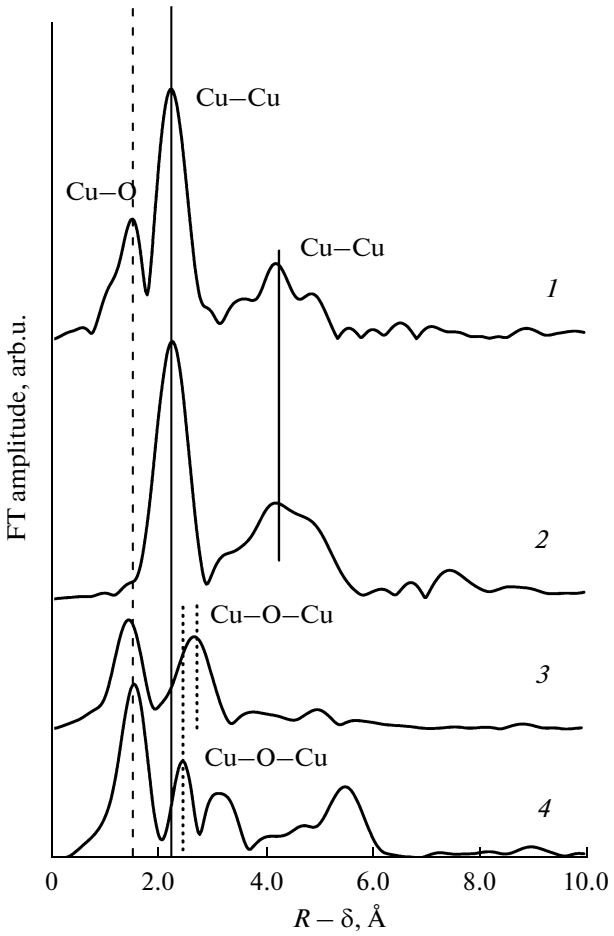

Fig. 7. Atomic radial distribution functions for the local environment of copper atoms in (*1*) 2L-FH(Cr9Cu7) after the reaction at 340°C and (*2–4*) reference materials: (*2*) Cu foil, (*3*) Cu_2O, and (*4*) CuO (R = distance, δ = phase correction).

The high activity of the copper-containing catalysts at low temperatures is likely due to the copper sites. At higher temperatures, the copper sites undergo deactivation, possibly via their oxidation by the water vapor present in the reaction mixture, and the catalytic activity is determined only by iron sites.

XAFS data suggest that the copper cations promoting 2L-FH are in the Cu^{2+} state and in a tetrahedrally distorted octahedral environment (tetragonal bipyramid); under the WGS conditions, they are in the reduced state, specifically, in the form of ultrafine (<2 nm) Cu^0 particles. It is due to these particles that the catalyst shows high activity at low temperatures.

ACKNOWLEDGMENTS

The authors are grateful to Candidate of Physics and Mathematics V.I. Zaikovskii, M.P. Demeshkina, and A.V. Kuznetsova for their assistance.

This study was supported by the Presidium of the Russian Academy of Sciences (program nos. 7.14 and 24.12), by the Russian Foundation for Basic Research (grants NSh-3156.2010, 120301154, and 120301039),

Table 5. Steady-state rate constants of the WGS reaction at 330°C over 2L-FH(Cr9Cu7) HCCPs pre-heat-treated at 480°C in the reaction medium

Material	k, s^{-1}	
	before heat treatment	after heat treatment
2L-FH(Cr9Cu7)	25.0	4.1
Hem-Fe	2.6	2.6

Table 6. Steady-state rate constants of the WGS reaction at 340°C over catalysts pre-heat-treated at 480°C in the reaction medium

Catalyst	S_{sp}, m^2/g	AS, m^{-2}	k_{340}, s^{-1}	Activity, $cm^3\ s^{-1}\ AS^{-1}$
2L-FH	41	1.2×10^{18}	1.6	3.9×10^{-20}
2L-FH(Cr9Cu7)	8	1.1×10^{18}	3.5	3.3×10^{-20}
2L-FH(Cr7)	67	1.0×10^{18}	1.8	3.3×10^{-20}
Goeth-Fe	63	1.0×10^{18}	0.5	3.9×10^{-20}

and by the Ministry of Education and Science of the Russian Federation (contract no. 16.518.11.7019).

REFERENCES

1. Chuckrov, F.V., Zvyagin, B.B., Gorshov, A.I., Yermilova, L.P., and Balashova, V.V., *Int. Geol. Rev.*, 1973, vol. 16, p. 1131.
2. Yu, J.Y., Park, M., and Kim, J., *Geochem. J.*, 2002, vol. 36, p. 119.
3. Jambor, J.L. and Dutrizac, J.E., *Chem. Rev.*, 1998, vol. 9, p. 2549.
4. Khassin, A.A., Minyukova, T.P., Plyasova, L.M., Filonenko, G.A., and Yurieva, T.M., *Advances in Nanotechnology*, Bartul, Z. and Trenor, J., Eds., New York: Nova Science, 2010, vol. 2, p. 347.
5. WO Patent Appl. 0189686, 2001.
6. WO Patent, Appl. 03043734, 2003.
7. Khassin, A.A., Sipatrov, A.G., Demeshkina, M.P., and Minyukova, T.P., *React. Kinet. Catal. Lett.*, 2009, vol. 97, p. 371.
8. Zhao, J.M., Feng, Z., Huggins, F.E., and Huffman, G.P., *Energy Fuels*, 1994, vol. 8, no. 5, p. 1152.
9. US Patent 5580839, 1996.
10. Tabakova, T., Andreeva, D., Idakiev, V., and Andreev, A., *J. Mater. Sci.*, 1996, vol. 31, p. 1101.
11. Khassin, A.A., Minyukova, T.P., Demeshkina, M.P., Baronskaya, N.A., Plyasova, L.M., Kustova, G.N., Zaikovskii, V.I., and Yurieva, T.M., *Kinet. Catal.*, 2009, vol. 50, no. 6, p. 837.
12. RF Patent 2314870, 2008.
13. Vishnevskii, A.L., Molchanov, V.V., Krieger, T.A., and Plyasova, L.M. *Int. Conf. on Powder Diffraction and Crystal Chemistry*, St. Petersburg, 1994, p. 208.
14. Binsted, N., Campbell, J.V., Gurman, S.J., and Stephenson, P.C., *EXCURV92 Program Code*, Daresbury, UK: SERC Daresbury Laboratory, 1991.
15. Baronskaya, N.A., Minyukova, T.P., Sipatrov, A.G., Demeshkina, M.P., Khassin, A.A., Dimov, S.V., Kozlov, S.P., Kuznetsov, V.V., Terentiev, V.Ya., Khristolyubov, A.P., Brizitskiy, O.F., and Yurieva, T.M., *Chem. Eng. J.*, 2007, vol. 134, p. 195.